Chapter 3

Method of Synthesis and Characterisation

3.1. Introduction

Characterization techniques are used to probe and measure the structure, composition of the material and properties of materials. The several spectroscopic experimental technique has been used to the thesis related work like X-Ray Diffraction, Fourier transform infrared (FT-IR) spectroscopy, Ultraviolet and Visible (UV-Vis) absorption spectroscopy, Photoluminescence (PL) spectroscopy, Raman spectroscopy, X-ray photoelectron spectroscopy (XPS) , Dynamic light scattering (DLS),Transmission electron microscopy (TEM),Scanning Electron Microscopy(SEM). Brief introduction of them has been discussed in below. The required material and method of synthesis of our produced material also has been described.

3.1.1. X-Ray diffraction (XRD)

It is a technique to determine atomic and molecular structure of crystalline material. The atomic planes of the crystalline material diffract X-rays in different specific directions depending on their orientation. X-ray diffraction is based on crystalline sample and constructive interference of monochromatic X-rays. X-rays are created by a cathode ray tube and filtered to generate monochromatic radiation, collimated to concentrate, and directed toward the material. When the conditions satisfied of Bragg's Law ($n\lambda=2d\sin\theta$), then the interaction of the incident radiation with the sample generates a constructive interference (and a diffracted ray). The Braggs law relates the lattice spacing in a crystalline material, the diffraction angle and the wavelength of electromagnetic radiation. The spectra consist of different components, K_α and K_β are the most common. Kα consists of two part (Kα1 and Kα2). Kα1 has twice of intensity than Kα2. Also, Kα1 has a slightly shorter wavelength than Kα2. The specific wavelengths depend of the target material (Cu, Fe, Mo, Cr etc). The peak with intensity and the constructive interference appeared when the geometry of the incident

X-rays impinging on the material satisfies the Bragg Equation. A detector collects and converts the X-ray signal to a count rate which is then forms and output to a device. The average particle size (D) of the crystalline material can be determined by observing the width of the diffraction peak and using the equation, known as Debye-Sherrer equation $D = 0.9\lambda / (\beta \cos \theta)$ (1.1) where, β is the full with at the half maximum (FWHM), θ is the diffraction angle and λ is the X-ray wavelength [1]. The geometry of an X-ray diffractometer is such that the sample rotates in the path of the collimated X-ray beam with an angle θ while the X-ray detector is mounted on an arm to record the diffracted X-rays and rotates at an angle of 2θ. Because of the presence of polycrystalline diffracting domain aggregates, crystallite size may not be the same as particle size.

3.1.2. Fourier transform infrared (FT-IR) spectroscopy

FT-IR spectroscopy is one of the most common spectroscopic techniques, which study the interactions between matter and electromagnetic (EM) fields in the infrared region (IR) .According to first approximation, the sum of vibrational, rotational, vibrational and electronic energy levels of a molecule is the the total internal energy of the molecule. In this spectroscopic technique, a molecule can be excited to a higher vibrational state by absorbing IR radiation. An FT-IR spectrometer simultaneously collects spectral data in a wide spectral range which can be categorized as far infrared (4 ~ 400 cm-1), mid infrared (400 ~ 4,000 cm-1) and near infrared (4,000~ 14,000 cm-1) and it is the absorption measurement of different IR frequencies by a sample positioned in the path of an IR beam. The functional groups present in the sample can be understood by the characteristic frequencies of the different functional groups absorbed by IR radiation. FT-IR spectrometers can accept a wide range of sample types which include solids, gases and liquids by using different sampling accessories. So, FT-IR spectroscopy is important tools for structural elucidation and compound

identification [2]. The FTIR spectra were recorded using FTIR-680 plus (Jasco) at room temperature.

3.1.3. Ultraviolet and Visible (UV-Vis) absorption spectroscopy

This spectroscopy refers to absorption spectroscopy in the ultraviolet visible spectral region and it uses electromagnetic radiation in the region of visible and adjacent (near-UV and near infrared [NIR]) range. In this region of the electromagnetic spectrum, molecules undergo electronic transitions from the ground state to the excited state by absorption of light. So, this technique is complementary to fluorescence spectroscopy whic deals with transitions from the excited state to the ground state. Molecules which has π-electrons or non-bonding electrons (n-electrons) can absorb the energy in the form of ultraviolet/visible light and these electrons are excited to higher energy molecular orbitals. When, the lower is energy gap, the electrons are more easily excited i.e. the longer the wavelength of light is absorbed. UV-Vis spectroscopy provides a relatively easy and effective technique for quantitatively characterizing both inorganic and organic materials. The-Beer Lambert Equation [equation (i)] is used for quantitative determination of concentration of an absorbing species in a solution to characterize the sample.

$$A = \log I_0/I = \varepsilon CL \quad \ldots\ldots\ldots\ldots \text{(i)}$$

Where I_0 is the intensity of the incident light at a given wavelength,

I is the transmitted intensity.

A is the measured absorbance.

L is the path-length through the sample

ε is the molar extinction coefficient.

For a particular sample, the absorption spectrum is the plot of amount of radiation absorbed versus wavelength is called as absorption spectrum. Thus, UV-Vis absorption spectroscopy is

very important technique which used to study the electronic and optical properties of the materials [3]. Absorption spectra were recorded on a Hitachi U-4010 spectrophotometer at room temperature.

3.1.4. Photoluminescence (PL) spectroscopy

The excitation by light (photon) of an atomic or molecular system which emits a portion of the excitation energy as a photon of another colour known as Photoluminescence (PL). PL processes are classified as fluorescence and phosphorescence.PL process can be explained by a Jablonski diagram .The singlet energy states as indicated by S_0, S_1, and S_2 corresponds to ground state, first excited state and second excited state respectively. The vertical lines indicates the transition from the ground state to the higher energy state of light absorption process. Excitation by light (photon) due to large gap between the ground states and the excited states instead of thermally induced excitation at room temperature. The fluorophore is excited by the absorption of light at a higher energy state S1 or S2, and then rapidly (< 10-12 s) relax to the lowest allowed energy level of S1 through a process called internal conversion. If the excited fluorephore emits is excited energy by radiative pathway with the emission of photon at a longer wavelength to the ground singlet energy the ground states, called fluorescence. This spectral shift is known as Stokes shift. The phosphorescence is a similar process like fluorescence except the excited electrons at S_1 can undergo a intersystem crossing to a forbidden triplet state T_1 and then relax its energy from triplet T_1 to the ground singlet states S_0 , as a result, the relaxation from triplet states takes longer than the fluorescence process and has a longer wavelength emission.

The major advantages of photoluminescence are:

1. Analysis of photoluminescence helps to understand the mechanism behind the recombination processes

2. Identification of impurity levels, surface and interface

3. By quantifying the amount radiative recombination, material quality can be understood.

4. Radiative recombination may also involve localized defects and the photoluminescence (PL) energy corresponding to these state, which may provide information regarding these specific defects. Thus, it helps to detect the impurity and defect level of the material.

5. Measurment of fluorescence lifetime i.e. the time a fluorophore spends in the excited state before returning to the ground state by emitting a photon help us to understand the number of component present within the sample. [4].

The steady state fluorescence and fluorescence excitation spectra were measured using a Hitachi Model F-7000 spectrofluorimeter equipped with a 150-W xenon lamp.

3.1.5. Fluorescence Life Time

The lifetimes of fluorophores can range from picoseconds to hundreds of nanoseconds. The fluorescence lifetime is a measure of the time a fluorophore spends in the excited state before returning to the ground state by emitting a photon.

The fluorescence lifetime was measured by using TCSPC from PTI, USA, with the support of subnanocond pulsed LED source (280 nm having a pulse width of 600 ps). The pulsed LED source of 280 nm was functioned at 10 MHz repetition rate driven by a PDL 800-B driver, PicoQuant, Germany. LED profile was estimated at the excitation of 280 nm with a band pass of 3 nm using Ludox as the scatterer. Decay measurements using "magic angle" detection with an emission polarizer set at 54.7° were measured. The decay parameters were determined using nonlinear iterative fitting procedure based on the Marquard algorithm [5].

3.1.6. Raman spectroscopy

In this technique, a monochromatic laser is shone onto the sample surface and the molecules are excited by the monochromatic laser with frequency ν_0 and the molecule goes to a virtual energy state from the ground state. The excited molecules return to a different rotational or vibrational state by emitting light. During emitting, three different frequencies may obtained depending on the change in energy between the original state and resulting state.

1. When the molecule is excited by absorbing a light with frequency ν_0 and returned back to the same basic vibrational state. This type of elastic scattering of the photon is called Rayleigh scattering.

2. After absorbing a photon with frequency $\nu_{0,}$ if the vibrational energy of the molecule is increased, then the energy of the scattered photons is decreased with a down-shifted

frequency (longer wavelength) as the part of the photon's energy is transferred to the Raman-active mode. This type of inelastic scattering is called Stokes scattering.

3. After absorbing a photon with frequency $v_{0,}$ if the vibrational energy of the molecule is decreased, the energy of the scattered photons is increased with an up-shifted frequency (shorter wavelength) as the excessive energy of the excited Raman-active mode is released. This inelastic scattering is called anti-Stokes Scattering. [6-7].

3.1.7. Scanning Electron Microscopy

SEM is a imaging technique which is widely used material science. In this microscopic imaging technique, electron beam is used instead of light to form an image. SEM has many advantages such as higher resolution, large depth of field, and more control in the degree of magnification [8], and used in fracture characterization, thin film evaluation, microstructure studies, surface contamination examination etc. In this technique, the electron gun in an evacuated column above the sample surface produces a high-energy electron and when the electron beam focuses onto the target surface of a sample, the electrons interact with the surface atoms and generate a variety of electronic signals and generates a image about the surface of the sample.

3.1.8. Transmission electron microscopy (TEM)

This is a imaging technique in which a beam of electrons is transmitted through an ultra-thin specimen and interacted with the specimen. In this technology, the beam of electron of very short wavelength emitted from a gun at the top of a cylindrical column which has 2 meter high. To avoid the collision of electrons with air molecules, the vacuum must be required by evacuating the air from the column. The magnetic coils are placed at specific intervals and these magnetic coils are focusing the electron beam. So, the coils act as an electromagnetic condenser lens system. The heated filament produced the electrons and accelerated with an anode voltage. A higher anode voltage will increased the speed of the

electrons i.e. smaller de Broglie wavelength is obtained according to the equation, $\lambda = h/m\upsilon$. The wavelength of radiation is directly related to the resolving power of a microscope which is used to create an image. When the wavelength is decreased, the resolution power is increased. Thus, the accelerating voltage of the electron beam increases the resolution of the microscope. When, the electrons is transmitted through the specimen which causing interaction with the specimen and forms an image. The obtained image is magnified and focused onto an imaging device. A CCD camera may also used for detecting magnified image. Thus, TEM technology provide structural and morphological information of the material through high resolution imaging (HRTEM) [9]

3.2. Synthesis of Graphene Based Material

In the experimental section of the thesis related resesearh work, we have synthesised different graphene based material. They are given below and discussed with the details method of synthesis.

(i) Synthesis of Graphene Oxide (GO)

(ii) Synthesis of Graphene Oxide Polyaniline Nano Composite (GO-PANI)

3.2.1. Materials

Powdered flake graphite was purchased from Sigma-Aldrich. Aniline (Merck) was used without purification. Ammonium persulphate (APS, Rankem chemicals) has been used as a radical oxidant for polyaniline (PANI), , $NaNO_3$, $KMnO_4$, H_2SO_4 (98%) H_2O_2, were purchased from Merck as analytical pure reagents. All aqueous suspensions were prepared in double distilled deionized water.

3.2.2. Synthesis of GO

The graphene oxide (GO) has been synthesised on the basis of modified Hummer's method [10-11]. The concentrated H_2SO_4 (100 ml) was added to a mixture of graphite flakes (4.0 g) and $NaNO_3$ (1.0 g) and then continuously the resulting mixture was stirred at about

0°C maintained by keeping it in an ice-bath. Then 12 gm solid $KMnO_4$ was stepwise added and kept under vigorous stirring for 6 hours. The temperature of the mixture was about 20°C. Next, an additional $KMnO_4$ (12.0 g) was added at a time with stirring for 12 hours at room temperature. Then about 600 ml of ice-cold water was added slowly to the mixture with the addition of 30% H_2O_2 drop wise to reduce the excess $KMnO_4$ to stop the further oxidation. The mixture was then purified by washing with 5% HCl and warm water. The obtained mass was dried and dispersed in distilled water by 1 hour sonication. Then the large heavy particle was removed by centrifuging the dispersion at 5000 rpm for 30 minutes. Then the resulting supernatant liquid was filtered through 0.45 μm pore size membrane and again it was washed with 50% ethanol to isolate GO mass. The obtained mass was dried under vacuum at 60°C and collected solid brown product as pure GO which was dispersed in water by sonication and used for spectroscopic study.

3.2.3. Synthesis of GO-PANI

The solid GO has taken, which has been synthesised by modified Hummer's method [10-11]. GO-PANI composites have been prepared by the dispersion of aniline (10.2mg, 0.11 mmol) and required amount of GO (102 mg, GO: Aniline weight ratio = 10:1) in water with sonication for 1 hour followed by stirring for 1 hour to make the dispersed solution. Then the mixture was cooled at 10^0 C. Aqueous solution of ammonium persulphate (APS, 1.1 mmol) was added very slowly over 30 min and the mixture was allowed to stand for 24 hrs at low temperature. The resultant precipitate was filtered and washed several times with water and methanol. Finally, it was dried under vacuum for 48 hrs at room temperature.

3.3. Characterisation Technique

Synthesized nanomaterial have been characterised by Raman spectrum, FT-IR spectrum, X-ray diffraction study, scanning electron microscopy (SEM) and transmission electron microscopy (TEM).

3.3.1. Characterisation of GO

Raman spectroscopy is a very useful technique to obtain the structural information of graphitic carbon-based materials. In the Raman spectra, the main characteristics features of graphitic carbon-based materials are the most intense G and D band. The observation of G band is due to the first order scattering of E_{2g} mode, related to sp^2 domains due to vibrations of hexagonal lattice of GO and this band near at 1600 cm^{-1} is the characteristic of graphene-like "honeycomb" structure [12]. The D band is due to associated with the reduction in size of the in-plane sp^2 domains, due to extensive oxidation.

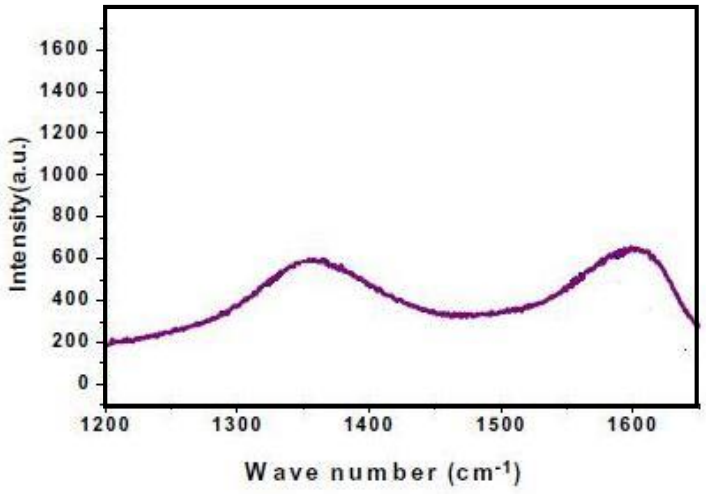

Fig. 1(a) Raman Spectrum of GO

Therefore, the D band of graphitic carbon material nearly appear at 1350 cm^{-1} and intensity of this band is often used to measure defect of the sample. In our GO sample, the Raman spectra [Fig.1(a)] shows the presence of a very strong D peak at ~1350 cm−1 with an intensity comparable to that of the G peak at ~1596 cm−1 and this spectra is a indicates of significant structural disorder due to the harsh oxidation condition in Hummer's process. The intensity ratio of the D band to G band (I_D/I_G) of our GO is about ~1 and this value is very close to the result obtained from GO from Ganguly et al. [13] and Wang et al. [14].

The FT-IR spectrum [Fig. 1b] indicates that the C=O groups present in the sample in the form of free carboxylic acid and also, the C=O groups present in the form of hydrogen bonded carboxylic acid moieties by showing two sharp peaks at 1726 and 1622 cm^{-1} respectively, due to the weakening of carbonyl bond by hydrogen bonding in the later case. A broad band having a center at ~ 3380 cm^{-1} is appeared mainly due to the stretching mode of vibration of the –OH functional group, which indicates that GO contains the numerous surface hydroxyl groups (-OH group).

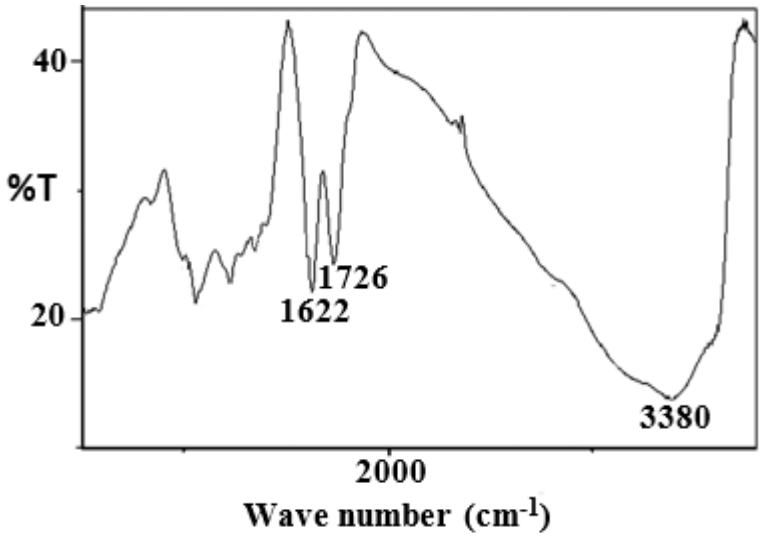

Fig. 1(b) FT-IR Spectra of GO

In our GO sample, the XRD spectra [Fig. 1c] shows a most intense sharp diffraction peak at 2θ= 7.97˚ corresponds to the (001) diffraction plane with an interlayer spacing of 1.11 nm.[12] The larger interlayer distance of GO from natural graphite flake might be due to the formation of hydroxyl, epoxy and carboxyl like oxygen-containing functional groups [15]. Another low intense peak appeared at 2θ= 25.97˚, this value is slightly lower than natural graphite flake which is due the the reflection of (002) plane. [16]

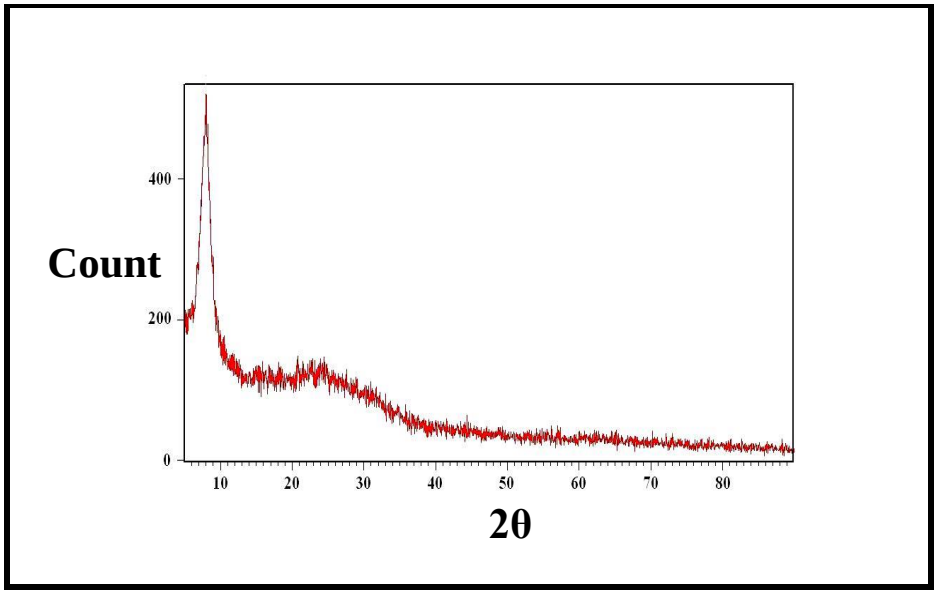

Fig. 1(c) X-ray diffraction Pattern GO

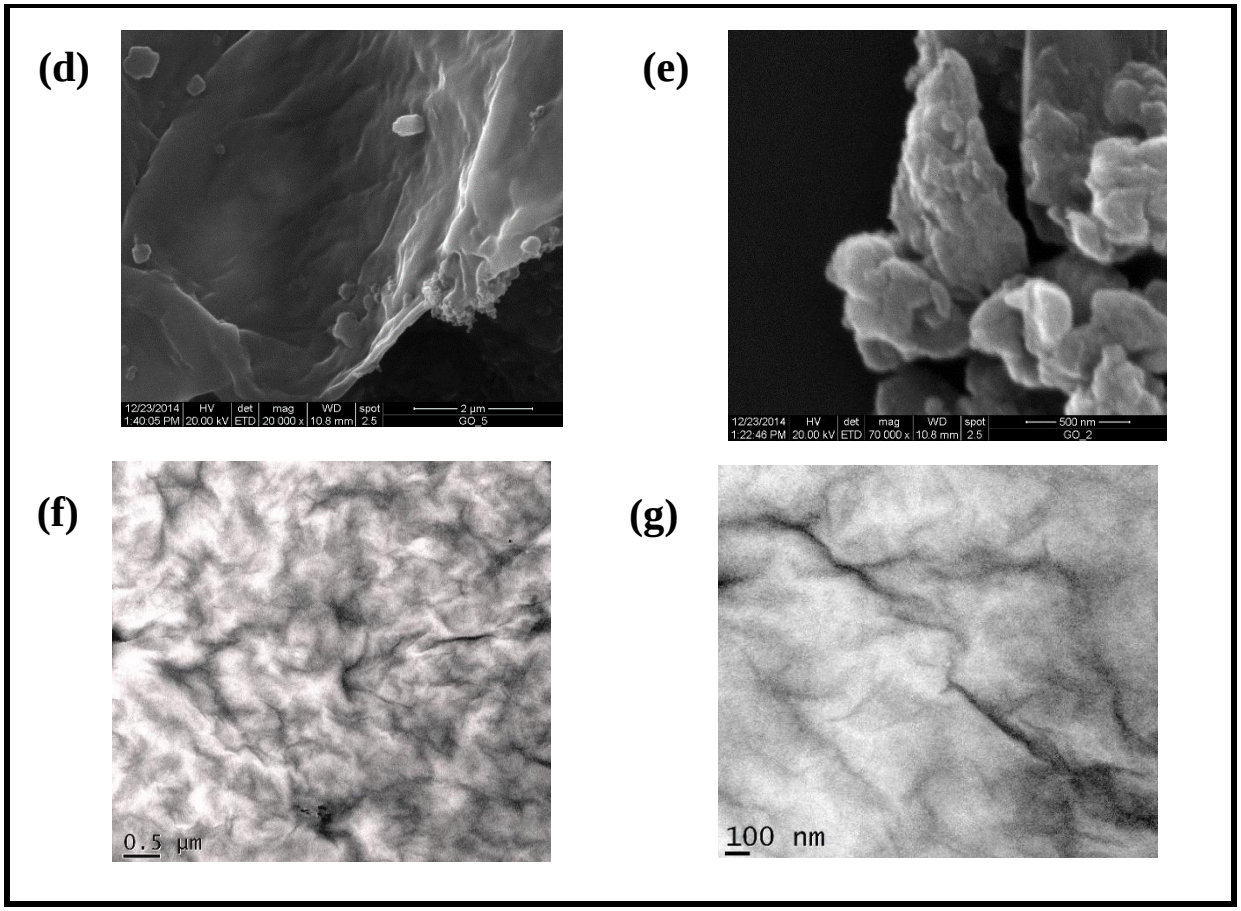

Fig-1 SEM image of GO (d) 2µm (e) 500 nm and TEM image of GO (f) 0.5 µm (g) 100 nm respectively.

The SEM and TEM images of GO displayed an exfoliated layer of several micrometres along with a curled morphology. The images are given above [Fig. 1(d), Fig. 1(e), Fig.1(f),Fig.1(g)]

3.3.2. Characterisation of GO-PANI

In the Raman Spectra of GO-PANI, two peaks appeared at 1350 cm^{-1} and 1590 cm^{-1} respectively and First one known as D band (disordered band) and later is G band (Growth band) [Fig. 2(a)].

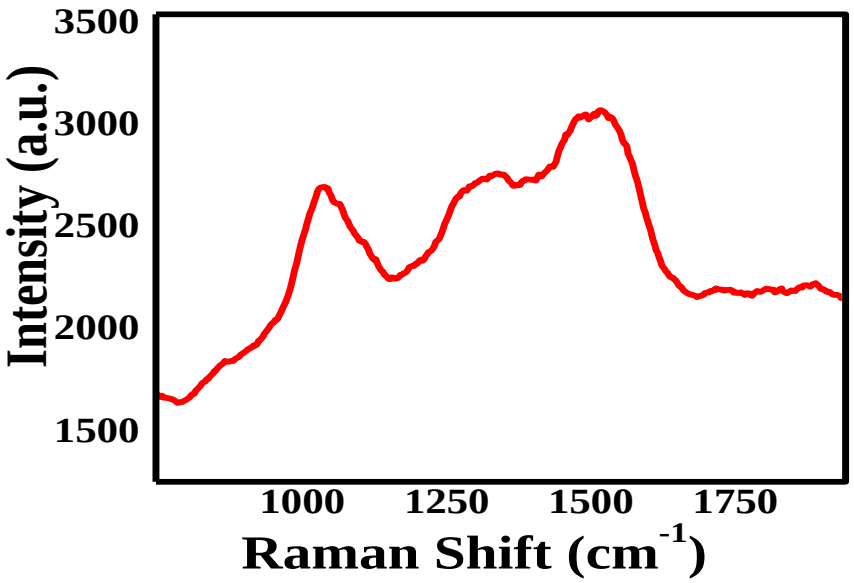

Fig. 2(a) Raman Spectrum of GO-PANI

The cause of the appearance of these band described in the Raman spectra of GO. In GO-PANI, intensity ratio of the two peaks, at 1390 cm^{-1} and 1570 cm^{-1} is lower than GO (about 0.9). In addition to these two band, another peak at 1095 cm^{-1} was observed. This observation may be explained as a down shifted of C-H bending of the quinoid benzenoid ring.

Fig. 2(b) is the FT-IR spectrum of GO-PANI. The presence of typical bands of GO in FTIR spectrum (Fig. 1b) at 1045, 1170, 1220, 1620 and 1724 indicates the presence of alkoxy C-O stretching, C-H in plane bending in aromatic ring, vibration of C-O in epoxy group, stretching of hydrogen bonded C=O carboxylic group and C=O stretching of carboxylic acid, respectively [12,17-20]. In FTIR spectrum of GO-PANI, the observed peaks at 1093, 1299, 1497, 1570 cm^{-1} can be assigned to the characteristic peak related to PANI in nanocomposites due to delocalization of electrons in PANI chains, C–N stretching near 2° amine, benzenoid and quinoid stretching respectively for PANI like characteristic peaks (Fig. 2b) [21,22]. Also, a peak at ~1045 cm^{-1} is observed which is due to alkoxy C-O stretching. Again, the peak at 1724 cm^{-1} which was appeared in GO, a characteristic of C=O stretching of carboxylic acid is disappeared in GO-PANI. The characteristic N-Q-N-Q band around 1150 cm^{-1} have also found with the observation of lower intensity of the quinoid band with respect to benzenoid band. Again, the shoulder at 1240 cm^{-1} may be attributed to the C-N stretching near the polaronic structure of emeraldine salt which has a small but finite contribution in the PANI.

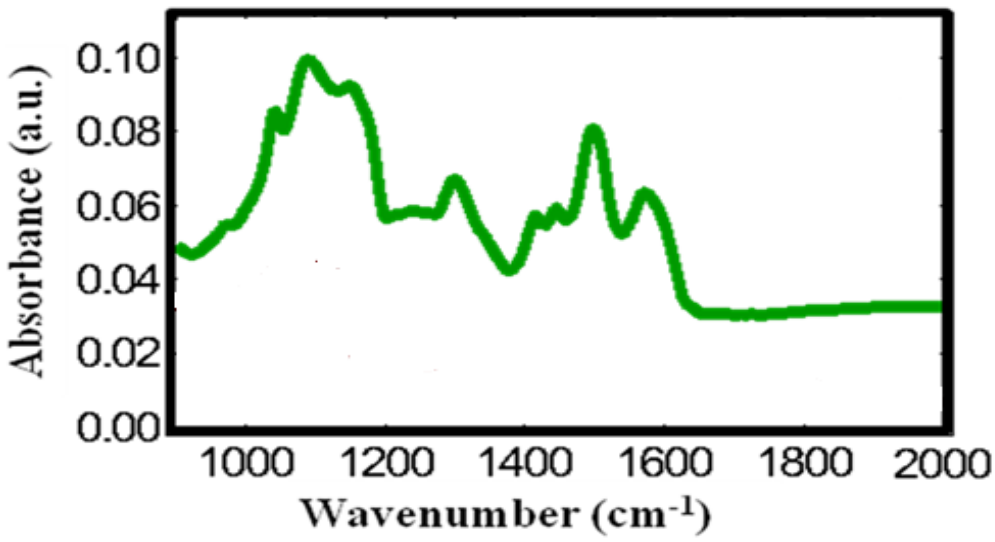

Fig. 2(b) FT-IR Spectra of GO-PANI

X-Ray diffraction spectrum of GO-PANI has been shown in Fig. 2(c). In the spectra, the characteristic peak of GO at $2\theta = 7.97^0$ corresponding to (001) reflection has been disappeared. Two characteristic peaks of PANI at $2\theta = 19.3^0$ (interplanar spacing = 0.46 nm) and $2\theta = 26^0$ (interplanar spacing = 0.343 nm) for 020 reflection and 200 reflection, respectively is observed [19, 22]. In addition to the two peak, a weak peak appeared at $2\theta = 7^0$ has also observed, which may be interpreted as little intercalation of PANI between the basal planes of GO by the reaction induced complete exfoliation of GO layers which makes larger interplanar distance [20, 23].

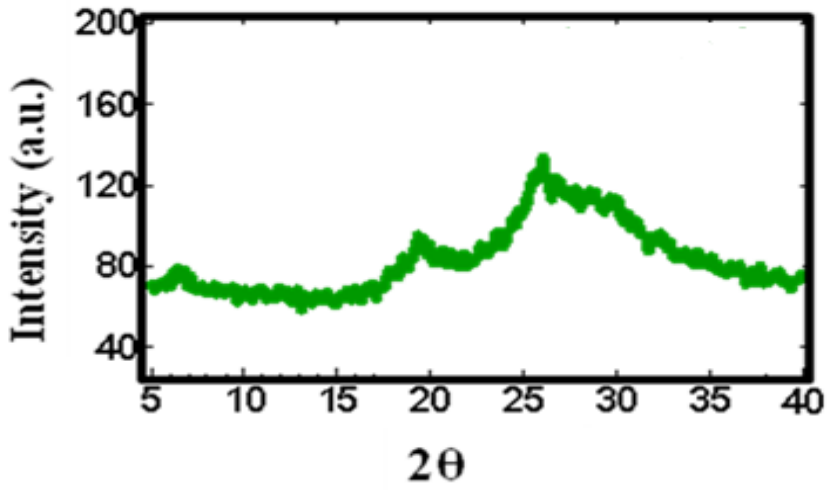

Fig. 2(c) Powdered XRD of GO-PANI (λ = 1.54 Å, Cu-Kα radiation)

The SEM image of GO-PANI [Fig. 2(d)] shows an irregular wrinkled fibriller morphology as observed by Kumar et al [19]. Careful observation of TEM images exhibits a curled morphology intrinsically associated with graphene due to disruption of the planar sp^2 carbon sheets by oxidation and some spots on the wrinkled structure [Fig. 2(e)] indicating the polycrystalline nature of the nanocomposites.

Fig. 2

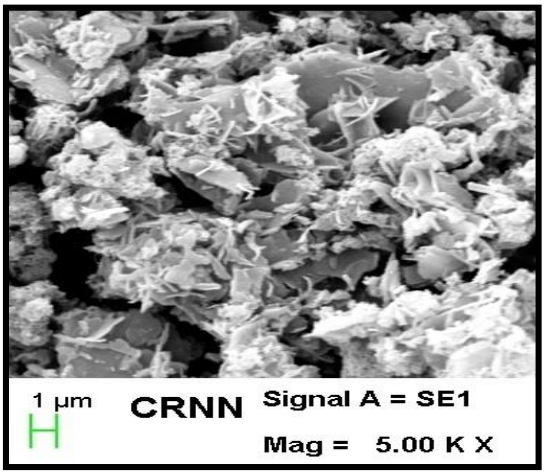

(d) SEM image of GO-PANI: 10 nm

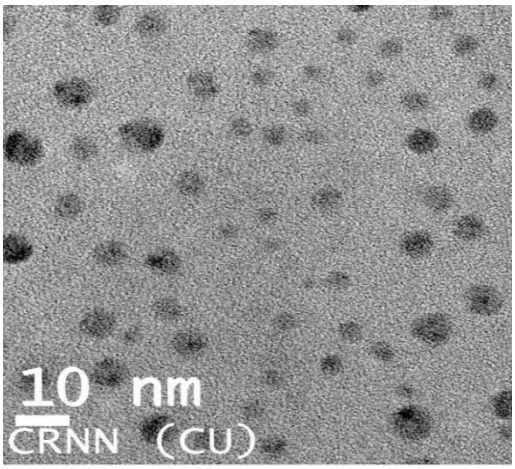

(e)TEM image of GO-PANI: 1µm

3.4. Reference

[1] B. D. Cullity and S. R. Stock, Elements of X-Rays Diffractions, 3rd edition, *Prentice Hall*, 2001.

[2] D. R. Lide, Handbook of Chemistry and Physics, 75th edition, *Boca Raton*, 1994.

[3] M. E. Malainey, Optical Spectroscopy, *Springer*, 2010.

[4] J. R. Deye, K. A. Walters, Photoluminescence and electro-luminescence, Encyclopedia of inorganic and bioorganic chemistry, 1 st edition, *Wily*, 2011.

[5] P. R. Bevington, Data Reduction and Error Analysis for the Physical sciences, *McGraw Hill, New York,* 1969

[6] D. Moss, Biomedical Applications of Synchrotron Infrared Microspectroscopy, *RSC*, 2011

[7] D. Tuschel, *Spectroscopy*, 2014, **29**, 110407-110412.

[8] Smith, W.F. and J. Hashemi, *Foundations of materials science and engineering*. 5th ed. 2010, Boston, Mass., *McGraw-Hill*., xviii, 1068.

[9] H. Ma, K. J. Shieh and T. X. Quiao, *Nat Sci*, 2006, **4**, 14-22.

[10] D. Nandi, K. Gupta, A. K. Ghosh, A. De, N. R. Ray, U. C. Ghosh, *Chem. Engin. J.*, 2013, **220**, 107- 116.

[11] D. C. Marcano, D. V. Kosynkin, J. M. Berlin, A. Sinitskii, Z. Sun, A. Slesarev, L. B. Alemany, W. Lu, J. M. Tour, *ACS Nano*, 2010, **4,** 4806- 4814.

[12] P. Dutta, D. Nandi, S. Datta, S. Chakraborty, N. Das, S. Chatterjee, U. C. Ghosh, A. Halder, *J. Lumin.* 2015, **168**, 269-275.

[13] A. Ganguly, S. Sharma, P. Papakonstantinou, J. Hamilton, *The Journal of Physical Chemistry C*, 2011, **115**, 17009–17019.

[14] S.J. Wang, Y. Geng, Q. Zheng, J.-K. Kim, *Carbon*, 2010, **48,** 1815–1823.

[15] S. Bykkam, V. K. Rao, S. CH. Chakra, T. Thunugunta, *Int. J. Adv. Biotech. and Research* 2013, **4**, 142-146.

[16] S. N. Alam, N. Sharma, L. Kumar, Scientific Research Publishing, *Graphene*, 2017, **6**, 1-18.

[17] S. M. Imran, Y. N. Kim, G. N. Shao, M. Hussain,Y. Choa, H. T. Kim, *J. Mater. Sci.*, 2014, **49**, 1328–1335.

[18] C. Vallés, P. Jiménez, E. Muñoz, A. M. Benito, W. K. Maser, *J. Phys. Chem. C*, 2011, **115**, 10468-10474.

[19] N. A. Kumar, H.-J. Choi, Y. R. Shin, D. W. Chang, L. Dai, J.-B. Baek, *ACS Nano*, 2012, **6**, 1715-1723.

[20] G. I. Titelman, V. Gelman, S. Bron, R. L. Khalfin, Y. Cohen, H. B**.** Peled, *Carbon***,** 2005, **43,** 641-649.

[21] A. A. Shyaa, O. A. Hasan, A. M. Abbas, *J. Saudi Chem. Soc.*, 2015**, 19,** 101-107.

[22] A. K. G. Tapia, K. Tominaga, *Chem. Phys. Lett.*, 2014, **598,** 39-42.

[23] Y.-Q. Li, T. Yu, T.-Y. Yang, L.-X. Zheng, K. Liao, *Adv. Mater*, 2012, **24**, 3426-3431.